

Published in final edited form as:

Nat Med. 2007 September ; 13(9): 1086–1095. doi:10.1038/nm1626.

Platelet CD36 links hyperlipidemia, oxidant stress and a prothrombotic phenotype

Eugene A Podrez¹, Tatiana V Byzova^{1,2,8}, Maria Febbraio^{3,8}, Robert G Salomon⁴, Yi Ma¹, Manojkumar Valiyaveetil¹, Eugenia Poliakov⁴, Mingjiang Sun^{3,5}, Paula J Finton³, Brian R Curtis⁶, Juhua Chen^{1,2}, Renliang Zhang^{3,5}, Roy L Silverstein³, and Stanley L Hazen^{3,5,7}

¹ Department of Molecular Cardiology, Cleveland Clinic Foundation, Cleveland, Ohio 44195, USA

² Joseph J. Jacobs Center for Thrombosis and Vascular Biology, Cleveland Clinic Foundation, Cleveland, Ohio 44195, USA

³ Department of Cell Biology, Cleveland Clinic Foundation, Cleveland, Ohio 44195, USA

⁴ Department of Chemistry, Case Western Reserve University, Cleveland, Ohio 44106, USA

⁵ Center for Cardiovascular Diagnostics & Prevention, Cleveland Clinic Foundation, Cleveland, Ohio 44195, USA

⁶ Platelet & Neutrophil Immunology Laboratory, Blood Center of Wisconsin, Milwaukee, Wisconsin 53233, USA

⁷ Department of Cardiovascular Medicine, Cleveland Clinic Foundation, Cleveland, Ohio 44195, USA

Abstract

Dyslipidemia is associated with a prothrombotic phenotype; however, the mechanisms responsible for enhanced platelet reactivity remain unclear. Proatherosclerotic lipid abnormalities are associated with both enhanced oxidant stress and the generation of biologically active oxidized lipids, including potential ligands for the scavenger receptor CD36, a major platelet glycoprotein. Using multiple mouse *in vivo* thrombosis models, we now demonstrate that genetic deletion of *Cd36* protects mice from hyperlipidemia-associated enhanced platelet reactivity and the accompanying prothrombotic phenotype. Structurally defined oxidized choline glycerophospholipids that serve as high-affinity ligands for CD36 were at markedly increased levels in the plasma of hyperlipidemic mice and in the plasma of humans with low HDL levels, were able to bind platelets via CD36 and, at pathophysiological levels, promoted platelet activation via CD36. Thus, interactions of platelet CD36 with specific endogenous oxidized lipids play a crucial role in the well-known clinical associations between dyslipidemia, oxidant stress and a prothrombotic phenotype.

An important role for increased platelet reactivity in the pathophysiology of occlusive arterial thrombi associated with myocardial infarction and stroke is widely recognized, and subjects with increases in various measures of platelet reactivity are at increased prospective

Correspondence should be addressed to E.A.P. (podreze@ccf.org).

⁸These authors contributed equally to this work.

Note: Supplementary information is available on the Nature Medicine website.

COMPETING INTERESTS STATEMENT

The authors declare no competing financial interests.

Reprints and permissions information is available online at <http://npg.nature.com/reprintsandpermissions>

risk for coronary events and death^{1–5}. Increased platelet reactivity and thrombogenic potential are associated with a number of pathophysiological states related to dyslipidemia, including atherosclerosis, diabetes, and metabolic syndrome^{2,6–10}. It has been suggested that the cardiovascular risk associated with dyslipidemia may be due at least as much to effects on thrombogenesis as to long-term effects on atherogenesis². The mechanisms responsible for enhancing platelet reactivity during dyslipidemia *in vivo* are still largely unknown, even though control of platelet reactivity is regarded as critical for prevention of coronary artery disease¹¹.

Dyslipidemia is associated with both oxidative stress and the generation of biologically active oxidized lipids. Moreover, enhanced platelet reactivity is associated with the accumulation of oxidized lipids in serum^{9,12–14}. Thus, oxidized lipids may be a link between hyperlipidemia and increased platelet reactivity. Biologically active oxidized phospholipids can initiate and modulate many of the cellular events attributed to the pathogenesis of atherosclerosis¹⁵. We have recently isolated and structurally defined a novel family of atherogenic oxidized choline glycerophospholipids (oxPC_{CD36}) that are formed during the oxidation of low-density lipoprotein (LDL) by multiple pathways¹⁶ and are present *in vivo* at sites of enhanced oxidative stress^{16–18}. oxPC_{CD36} serve as high-affinity ligands for the macrophage scavenger receptor CD36 (ref. ¹⁶) and facilitate macrophage foam cell formation through recognition and uptake of oxidized LDL by CD36 (ref. ¹⁹). CD36 is implicated in a variety of pathological conditions, including atherosclerosis, diabetes and innate immunity²⁰. Absence of CD36 in a mouse model of atherogenesis results in significant inhibition of atherosclerosis²¹.

Platelets express scavenger receptors, including CD36 (ref. ²²), although their functional role in platelet biology has not been defined. CD36 on macrophages and endothelial cells serves as a signaling molecule²⁰. We therefore hypothesized that interaction of oxPC_{CD36} with platelet CD36 may alter platelet reactivity, inducing prothrombotic signals associated with dyslipidemia. Here we show that interaction with oxPC_{CD36} results in enhanced platelet reactivity and a prothrombotic phenotype.

RESULTS

CD36 is involved in thrombosis *in vivo* during hyperlipidemia

To test the hypothesis that CD36 contributes to a prothrombotic phenotype under conditions of hyperlipidemia, we initially used a mesenteric thrombosis model and intravital microscopy to compare *in vivo* vessel occlusion times between age-matched groups of male mice fed a Western diet (Fig. 1). The time to thrombotic occlusion of mesenteric arterioles after induction of injury was significantly shorter in hyperlipidemic *ApoE*^{-/-} mice than in wild-type mice (Fig. 1a), indicating the presence of a pronounced prothrombotic phenotype. Notably, whereas functional deficiency of CD36 had no effect on thrombotic occlusion time in the absence of significant hyperlipidemia (compare wild-type to *Cd36*^{-/-} mice), the absence of CD36 in the *ApoE*^{-/-} background significantly protected mice from the hyperlipidemia-related prothrombotic phenotype (Fig. 1a). Parallel studies that quantified thrombotic occlusion times within venules demonstrated a similar distinct hyperlipidemia-related prothrombotic phenotype that was significantly rescued by CD36 deficiency (Fig. 1b). Notably, the absence of CD36 also protected mice from the hyperlipidemia-related prothrombotic phenotype state in carotid arteries—a large, atherosclerosis-prone vessel (Fig. 1c). Finally, hyperlipidemic *ApoE*^{-/-} mice had accelerated thrombosis in another model examined, tail-cut bleeding time (Fig. 1e). Again, the absence of CD36 markedly protected mice from the hyperlipidemia-associated prothrombotic phenotype (Fig. 1e). Differences in occlusion times observed in these experiments could not be explained by favorable changes in lipid profiles in *ApoE*^{-/-} *Cd36*^{-/-} mice as compared to *ApoE*^{-/-} mice (Fig. 1f) or by

altered platelet production, as platelet counts in *ApoE*^{-/-} *Cd36*^{-/-} mice ($4.01 \pm 0.88 \times 10^8$ /ml) were similar to those of *ApoE*^{-/-} mice ($4.13 \pm 0.72 \times 10^8$ /ml; $P > 0.5$). Because occlusion times in wild-type and *Cd36*^{-/-} mice were similar (Fig. 1a,b,e), differences in platelet-collagen interaction can also be ruled out as a potential contributor to the observed impact of CD36 deficiency on the hyperlipidemia-induced prothrombotic phenotype.

To assess whether the CD36-dependent effects described above were specific to the setting of hyperlipidemia, we performed occlusion assays in mice fed a chow diet using an increased duration of ferric chloride exposure that induced rates of closure comparable to those observed in mice on Western diet (Fig. 1a–c empty bars). Even though there was greater vessel damage in this series of experiments, the time to occlusion in most cases was increased as compared to Western diet–fed animals, indicating a lower prothrombotic potential in mice on chow diet. Notably, there was no statistically significant difference in the occlusion times in *ApoE*^{-/-} mice as compared with *ApoE*^{-/-} *Cd36*^{-/-} mice in all three types of vessel studied, consistent with our hypothesis that CD36-mediated effects are dependent on hyperlipidemia.

To address any potential issues related to the mixed genetic background of the *Cd36*^{-/-} and *ApoE*^{-/-} *Cd36*^{-/-} mice, we used independently generated, CD36-deficient ‘oblivious’ mice²³ that are pure C57BL/6. The occlusion times of *ApoE*^{-/-} oblivious mice and *ApoE*^{-/-} *Cd36*^{-/-} mice on Western diet were very similar (arterioles: 19.1 ± 7.0 min versus 22.3 ± 7.3 min; venules: 22.1 ± 6.4 min versus 21.8 ± 5.0 min; all values are means \pm s.d.). The occlusion times of oblivious mice and *Cd36*^{-/-} mice on Western diet were also similar (arterioles: 21.8 ± 8.8 min versus 24.9 ± 7.9 min; venules: 19.9 ± 8.6 min versus 20.8 ± 7.1 min; all values are means \pm s.d.).

To demonstrate that platelet CD36 was responsible for the observed differences, we first depleted *ApoE*^{-/-} and *ApoE*^{-/-} *Cd36*^{-/-} mice of platelets by γ -irradiation, then injected them intravenously with platelets from either *ApoE*^{-/-} or *ApoE*^{-/-} *Cd36*^{-/-} mice and then performed carotid artery occlusion assays. In all cases, both the donor and the recipient mice were maintained on a Western diet. The occlusion time was significantly longer when platelet donors were *ApoE*^{-/-} *Cd36*^{-/-} as compared to *ApoE*^{-/-} (Fig. 1d). This result was independent of the genotype of the recipient mice.

To demonstrate that the effect of CD36 deficiency was not restricted to hyperlipidemia associated with apoE deficiency, we employed another widely used model of murine hyperlipidemia: LDL receptor-deficient mice (*Ldlr*^{-/-}) fed a high-cholesterol diet. The lipoprotein profile in these mice is different from that of *ApoE*^{-/-} mice and is similar to that observed in humans with familial hypercholesterolemia. The time to thrombotic occlusion after induction of injury was significantly shorter in *Ldlr*^{-/-} mice than in wild-type mice in all three types of vessels examined (Fig. 1g). The absence of CD36 in the hyperlipidemic *Ldlr*^{-/-} background again significantly protected mice from the prothrombotic state (Fig. 1g). Taken together, these results demonstrate that platelet CD36 may have a disease-modifying role by reducing the hyperlipidemia-associated prothrombotic state, and that CD36 can contribute to thrombosis in various blood vessels, including large, atherosclerosis-prone arteries.

CD36 deficiency in hyperlipidemia modulates platelet reactivity

It has previously been reported that platelets from hyperlipidemic animals and humans have an increased *in vitro* aggregation response. To determine whether this augmented response was CD36 dependent, the aggregation of platelets in response to a suboptimal dose of adenosine diphosphate (ADP) was examined in different groups of mice. We observed a significant increase in the extent and rate of aggregation of platelets from hyperlipidemic

ApoE^{-/-} mice compared with wild-type mice (Fig. 2a). This response was significantly blunted in platelets from *ApoE*^{-/-} *Cd36*^{-/-} mice (Fig. 2a). No significant differences were observed between platelets from wild-type and *Cd36*^{-/-} mice on normal chow (data not shown), again indicating that CD36 plays an important modulatory role in platelet function only in the setting of hyperlipidemia. Similar results were obtained when platelets from hyperlipidemic *Ldlr*^{-/-} mice were compared to platelets from *Ldlr*^{-/-} *Cd36*^{-/-} mice (Fig. 2b).

Next, platelets from wild-type and *Cd36*^{-/-} mice on chow diet and from hyperlipidemic *ApoE*^{-/-} mice fed Western diet were separated from plasma by gel filtration, combined with citrated platelet-poor plasma from either wild-type or hyperlipidemic *ApoE*^{-/-} mice, and tested in an aggregation assay. The aggregation response of platelets from *ApoE*^{-/-} mice in plasma from wild-type mice was similar to that observed with platelets and plasma from wild-type mice (Fig. 2c,d). Platelet hyperreactivity was induced by adding hyperlipidemic plasma from *ApoE*^{-/-} mice to platelets isolated from either *ApoE*^{-/-} or wild-type mice (Fig. 2c,d). Thus, a factor present in the hyperlipidemic plasma was sufficient to confer a hypercoagulable (enhanced aggregation response) state. This effect required platelet CD36, because no enhanced aggregation was noted in *Cd36*^{-/-} platelets in the presence of hyperlipidemic (*ApoE*^{-/-}) plasma (Fig. 2c,d). In a parallel set of experiments, we found that activation of platelet fibrinogen receptor integrin $\alpha_{IIb}\beta_3$ in response to ADP was significantly increased in the presence of hyperlipidemic plasma, but only in CD36-expressing platelets (Fig. 2e). Notably, even without agonist added, a significant increase in the level of activated $\alpha_{IIb}\beta_3$ was observed when the platelets were incubated with hyperlipidemic plasma (Fig. 2e). These results demonstrate that the observed platelet hyperreactivity has a CD36 requirement and is associated with the presence of a procoagulant agent in hyperlipidemic plasma.

oxPC_{CD36} are markedly increased in hyperlipidemic plasma

Recent studies have reported the isolation and structural characterization of a novel family of oxidized choline glycerophospholipids (oxPC_{CD36}) that are enriched within atheromas and serve as specific high-affinity ligands for macrophage CD36 (refs. ^{16,17}; the structures and names of oxPC_{CD36} molecular species are shown at the top of Table 1). Because hyperlipidemia is associated with enhanced indices of oxidant stress, we hypothesized that oxPC_{CD36} species may accumulate in plasma during hyperlipidemic conditions, where they may serve as ligands for platelet CD36 and thereby modulate platelet reactivity.

Multiple structurally distinct and specific oxidized phospholipids in plasma samples of mice fed a chow diet or a diet enriched in cholesterol were quantified by liquid chromatography–electrospray ionization tandem mass spectrometry (LC/ESI/MS/MS) analyses. Significant increases in concentration (typically over an order of magnitude) of each of the CD36 ligands derived from the oxidation of 1-hexadecanoyl-2-eicosatetra-5',8',11',14'-enoyl-*sn*-glycero-3-phosphocholine (PAPC) and 1-hexadecanoyl-2-octadecadi-9',12'-enoyl-*sn*-glycero-3-phosphocholine (PLPC) were noted in hyperlipidemic *ApoE*^{-/-} and *Ldlr*^{-/-} mice, with the collective plasma concentration of oxPC_{CD36} molecular species exceeding 10 μ M (Table 1). Plasma levels of oxPC_{CD36} were not affected by the absence of CD36 in either the wild-type or the *ApoE*^{-/-} background ($P > 0.5$, data not shown).

oxLDL and oxPC_{CD36} bind to platelets through CD36

LDL oxidized by the myeloperoxidase-hydrogen peroxide-nitrite (MPO – H₂O₂ – NO₂⁻) system (NO₂-LDL) is a carrier of oxPC_{CD36} and represents an *in vivo*-relevant model of oxidized LDL that selectively binds to CD36 (refs. ^{16,17,19,24}). Platelets isolated from human blood bound significant amounts of [¹²⁵I]NO₂-LDL, whereas platelet binding of

native [^{125}I]LDL or acetylated [^{125}I]LDL (a ligand for the scavenger receptor class A) was low (Fig. 3a). LDL oxidized by alternative methods (for example, Cu^{2+} -mediated oxidation) also bound to platelets. Competition experiments demonstrated that [^{125}I]NO₂-LDL binding was highly specific and was mediated by oxidized lipids (data not shown). Substantial binding of [^{125}I]NO₂-LDL to platelets was observed in platelet-rich plasma (data not shown), indicating that NO₂-LDL can bind to platelets in conditions resembling those *in vivo*. [^{125}I]NO₂-LDL binding by isolated human platelets was saturable (Fig. 3b), with half-maximal binding observed at 6 $\mu\text{g}/\text{ml}$ (12 nM), indicative of a high-affinity interaction. The maximum amount of bound [^{125}I]NO₂-LDL corresponded to $\approx 26,000$ binding sites per platelet, which is close to the amount of CD36 on the surface of human platelets²⁵. An inhibitory monoclonal antibody to CD36, FA6, significantly blocked binding of [^{125}I]NO₂-LDL to platelets, whereas an isotype-matched non-immune antibody or antibody to an alternative major platelet glycoprotein, $\alpha_{\text{IIb}}\beta_3$, had no effect (Fig. 3c). [^{125}I]NO₂-LDL binding to wild-type mouse platelets was significantly higher than that to *Cd36*^{-/-} mouse platelets (Fig. 3d). In contrast, binding of native [^{125}I]LDL to platelets from wild-type or *Cd36*^{-/-} mice was low in both cases. Collectively, these results are consistent with platelet recognition of NO₂-LDL through a specific and saturable process mediated by CD36.

We next used a competition assay to examine whether the PAPC and PLPC preparations oxidized by the $\text{MPO} - \text{H}_2\text{O}_2 - \text{NO}_2^-$ system (NO₂-PAPC and NO₂-PLPC), as well as the individual structurally defined oxPC_{CD36} shown to be enriched within plasma of hyperlipidemic mice (Table 1), serve as ligands for platelet CD36. oxPC_{CD36} (data for HOdiA-PC are shown), NO₂-PAPC and NO₂-PLPC were all shown to completely inhibit [^{125}I]NO₂-LDL binding to platelets, whereas native PAPC or PLPC vesicles had no effect (Fig. 3e and data not shown). To directly demonstrate that oxPC_{CD36} bind to platelets via CD36, small unilamellar vesicles containing a carrier phospholipid and low mole percent synthetic oxPC_{CD36} species were made. Vesicles containing oxPC_{CD36} readily bound to platelets in a CD36-dependent manner; in contrast, vesicles containing only native PAPC or PLPC bound weakly (Fig. 3f). Thus, CD36 on both human and mouse platelets is important in the recognition of oxidized lipoproteins through its binding of specific oxidized phospholipids formed by physiologically relevant oxidation pathways.

oxPC_{CD36} induce platelet activation in a CD36-dependent manner

Having shown that oxidized LDL and oxPC_{CD36} bind platelets via CD36, we next tested whether this interaction could induce platelet activation. Platelet activation is characterized by a conformational change in the integrin $\alpha_{\text{IIb}}\beta_3$, enabling fibrinogen binding and platelet aggregation. We found that NO₂-LDL, NO₂-PAPC and NO₂-PLPC all induced platelet binding of fibrinogen comparable to that induced by the physiological platelet agonist ADP, whereas native LDL or unoxidized phospholipids had no effect (data not shown). We showed that pure synthetic individual oxPC_{CD36} induced $\alpha_{\text{IIb}}\beta_3$ activation of fibrinogen binding in a concentration-dependent manner by two independent methods (by assessing the platelet binding of [^{125}I]fibrinogen and the binding of FITC-labeled monoclonal antibody PAC-1 that is specific for activated integrin $\alpha_{\text{IIb}}\beta_3$) (Fig. 4a,b). The (patho)-physiological relevance of oxPC_{CD36}-dependent platelet activation was underscored by the observation that activation occurred at oxPC_{CD36} concentrations within the range seen during hyperlipidemia *in vivo* (Fig. 4a,b; data for KODA-PC, one of the oxPC_{CD36} species, are shown; compare with data in Table 1). As a control, parallel studies used oxovaleroyl phosphatidylcholine (OV-PC), a structural analog of oxPC_{CD36} and biologically active phospholipid formed during PAPC oxidation²⁶ for which no CD36 binding activity has been observed when it is presented in free, non-protein-bound form¹⁶ (notably, OV-PC as a protein adduct acquires the ability to bind to CD36; ref. ²⁷). Platelets exposed to OV-PC were not activated, even at high concentrations of OV-PC (Fig. 4a,b).

Although human $CD36^{-/-}$ platelet responses to multiple agonists, including ADP, thrombin and phorbol 12-myristate 13-acetate (PMA), were indistinguishable from those of CD36-expressing platelets, no activation of $\alpha II_b \beta_3$ was observed in platelets from CD36-deficient donors in response to 0.5–20 μM of oxPC_{CD36} (data for 20 μM is shown) (Fig. 4c). This specific lack of response to oxPC_{CD36} was also reproduced with platelets isolated from $Cd36^{-/-}$ mice as compared to those from wild-type mice (Fig. 4d).

Another critical component of platelet activation is the secretion of granular contents, a process that exposes P-selectin on the platelet surface. Platelet P-selectin mediates the formation of platelet-monocyte aggregates, which have been implicated in several vascular disease processes^{28–30}. NO₂-LDL, NO₂-PAPC and NO₂-PLPC vesicles were all potent inducers of P-selectin expression (Fig. 5a). oxPC_{CD36} (data for HODA-PC, another type of oxPC_{CD36}, are shown), but not OV-PC, induced platelet P-selectin expression as potently as did ADP (Fig. 5a). Native LDL, PAPC and PLPC vesicles had no effect on P-selectin expression. Similar results were obtained using either washed platelets or platelet-rich plasma (data not shown). The CD36-dependence of these effects was confirmed using a recombinant human CD36–glutathione *S*-transferase fusion peptide corresponding to amino acids 5–143 of the extracellular domain of CD36 that was shown previously to bind oxLDL³¹. This peptide, but not a control peptide (93–120 amino acids), demonstrated high-affinity recognition of specific oxPC_{CD36} (Fig. 5b) and [¹²⁵I]NO₂-LDL, and it significantly inhibited the activation of platelets by oxPC_{CD36} (Fig. 5a).

CD36 was necessary for the induction of P-selectin expression by oxPC_{CD36}, as NO₂-PAPC and pure synthetic oxPC_{CD36} did not induce expression when CD36 was blocked by the Fab fragment of FA6 (Fig. 5c,d). Moreover, mouse and human $CD36^{-/-}$ platelets showed significantly reduced P-selectin exposure compared to CD36-expressing platelets in response to NO₂-LDL, NO₂-PAPC and pathophysiologically relevant levels of the prototypic oxPC_{CD36} KODA-PC (Fig. 5e,f).

oxPC_{CD36} in human plasma modulate platelet reactivity

We then sought to determine whether oxPC_{CD36} were present in human plasma and whether these amounts were sufficient to promote platelet activation. Under conditions developed to minimize oxidation of lipids during their isolation from plasma¹⁷, we quantified the amounts of multiple distinct oxidized phospholipids in normotriglyceridemic plasma samples from donors ($n = 24$) with a wide range of plasma LDL cholesterol (range of 36–243 mg/dl) recruited from a Preventive Cardiology Clinic. We detected substantial amounts of oxPC_{CD36} and its oxidation products (such as OV-PC and G-PC, the glutaric acid ester of 2-lyso-PC) in all samples. There was considerable interindividual variability in the amounts of the multiple oxPC_{CD36} species monitored, with the concentration of an individual oxPC_{CD36} species ranging from undetectable to 1.8 μM , and the combined oxPC_{CD36} concentration ranging from approximately 0.7 to 4.6 μM . The combined concentration of all oxidized phospholipids measured, including those that are products of oxPC_{CD36} degradation, ranged from 5.4 to 51 μM . Thus, the concentrations of oxPC_{CD36} in human plasma are precisely within the concentration range demonstrated to promote prothrombotic activity in both mice and humans. We then tested whether agonist-induced platelet P-selectin expression correlated with plasma levels of oxPC_{CD36}, as well as whether any observed correlation was CD36 dependent. The effect of plasma from multiple donors on agonist-induced P-selectin expression was assessed on platelets isolated from CD36-positive or CD36-deficient human donors. Considerable, reproducible variations in the plasma effect on platelet response to agonists were observed. Plasma samples that reproducibly supported the highest P-selectin expression in CD36-positive platelets had significantly higher concentrations of specific oxidized phospholipids (Fig. 5g, left graph), compared to plasma samples that reproducibly supported the lowest P-selectin expression. HODA-PC is shown as a characteristic example

of an individual oxPC_{CD36}; similar patterns were observed with virtually all oxPC_{CD36} (Fig. 5g, left graph). Notably, the responses of CD36-deficient platelets failed to correlate with plasma levels of oxPC_{CD36} (Fig. 5g, right graph). There was no correlation between the platelet response to agonists with the concentrations of two major unoxidized phospholipids in plasma, PAPC and PLPC (Fig. 5g and data not shown). In addition, total cholesterol in the plasma did not correlate with the platelet responses. These results are consistent with a role for circulating oxPC_{CD36}-platelet interactions as modulators of platelet responsiveness to physiological agonists.

We next tested whether oxPC_{CD36} levels in human plasma samples correlate with high-density lipoprotein (HDL) and LDL cholesterol levels. Although no significant correlations were noted between LDL cholesterol and oxPC_{CD36}, a highly significant correlation was noted between oxPC_{CD36} (both individually and in combination) and HDL cholesterol (Fig. 5h). Data for the relationship between HODA-PC and HDL is shown as a typical example; similar patterns were observed with virtually all oxPC_{CD36}. The Spearman correlation coefficient for HODA-PC was 0.622 ($P < 0.0006$), and that for combined oxPC_{CD36} was 0.522 ($P < 0.005$). HODA-PC concentrations were more than three times higher in plasma from subjects in the lowest HDL tertile, and combined oxPC_{CD36} concentrations were, on average, about 2.5 times higher. In contrast to the oxidized phospholipid data, the concentrations of unoxidized phospholipids (data for PLPC are shown) showed modest increases with increasing HDL concentration. These findings demonstrate that in relatively normolipidemic human plasma it is HDL, not LDL, that controls oxPC_{CD36} concentrations.

DISCUSSION

The present studies support a previously unknown role for platelet CD36 as a sensor of oxidative stress and modulator of platelet reactivity, activation and thrombosis under hyperlipidemic conditions *in vivo*. Whereas macrophage CD36 involvement in fatty-streak formation and atherogenesis is well described^{19,21,32}, the involvement of this receptor in platelet function has not to our knowledge been unequivocally shown. Multiple studies have shown that dyslipidemia, a major risk factor for atherosclerosis, is associated with enhanced platelet reactivity and increased thrombogenic potential^{2,7,8,10}. The studies reported herein demonstrate that the engagement of platelet CD36 by structurally defined endogenous ligands plays a causal role in facilitating the development of a dyslipidemia-associated prothrombotic state.

Using two different mouse models of hyperlipidemia and several assays for *in vivo* thrombosis, we confirmed that hyperlipidemia induces a pronounced prothrombotic state; these findings are consistent with prior observations in *ApoE*^{-/-} mice^{33,34}. The present study markedly extends the analysis of this phenomenon by identifying a specific platelet receptor (CD36) and specific endogenous lipid ligands associated with oxidant stress (oxPC_{CD36}) as participants in this important pathophysiologic process. The observation that CD36-positive platelets in hyperlipidemic plasma showed increased aggregation responses at suboptimal agonist concentration *in vitro* provides a direct link between accelerated thrombosis and platelet thrombogenic status. There was no significant reduction in response to the agonist in platelets from *Cd36*^{-/-} mice as compared to wild-type mice on a normal chow diet, in line with our hypothesis that the role of CD36 in thrombosis is restricted to the dyslipidemic milieu, where there is enhanced oxidative stress that can generate specific ligands for CD36 (ref. 17). Furthermore, rescue of the hyperlipidemia-induced prothrombotic phenotype by *Cd36* deletion was observed in mesenteric arterioles and venules as well as in carotid arteries, indicating that this pathway contributes to thrombosis at both low and high shear stress rates, and in both large and small vessels.

We previously identified a family of oxidized choline glycerophospholipids with an *sn*-2 acyl group that incorporates a structural motif for supporting high-affinity CD36 recognition, a terminal γ -hydroxy (or oxo)- α,β -unsaturated carbonyl (oxPC_{CD36}). oxPC_{CD36} are formed during LDL oxidation by multiple pathways, are present *in vivo* at sites of enhanced oxidative stress^{16–18} and promote foam cell formation through CD36 (refs. 16,17). We now extend these observations to demonstrate that oxPC_{CD36} accumulate in the plasma of hyperlipidemic mice at concentrations up to 40-fold higher than those found in normolipidemic mice, and that they are found in substantial amounts in human plasma.

To support our hypothesis that oxPC_{CD36} link dyslipidemia and enhanced platelet reactivity, we demonstrated that various forms of oxLDL and multiple structurally specific oxPC_{CD36} (but not structural oxPC analogs lacking CD36 binding activity) bound to human and mouse platelets, and that binding was dependent on CD36. Ligand binding to platelet CD36 resulted in platelet activation, as assessed by activation of integrin $\alpha_{IIb}\beta_3$ as well as by an increase in P-selectin surface expression. The physiological relevance of these results is further supported by (i) the finding that oxPC_{CD36} levels in human and mouse plasma precisely span the concentration range in which biological effects on platelet responses are observed and (ii) the demonstration that a statistically significant correlation exists between the CD36-dependent platelet response to agonists and plasma levels of oxPC_{CD36}. Because anti-inflammatory and antioxidant effects of HDL are well documented³⁵, our finding of a link between elevated oxPC_{CD36} and low HDL suggests that it is an interaction between CD36 and oxidative stress, not merely dyslipidemia (or elevated LDL), that is responsible for enhanced platelet reactivity *in vivo*. It is thus tempting to speculate that individuals with high circulating plasma oxPC_{CD36} are at an increased risk for thrombosis.

CD36 is involved in a diverse array of physiological and pathological processes *in vivo*, including lipid sensing and metabolism, innate immune responses, angiogenesis, uptake of apoptotic cells, atherogenesis and diabetes^{20,23,36,37}. These various functional capacities arise as a result of the multiple distinct ligands with which CD36 interacts, the numerous downstream effectors upon which CD36 acts and the variety of cell types that express CD36. Surprisingly, even though CD36 was recognized as a major platelet glycoprotein more than three decades ago, its role in platelet physiology has remained obscure. Human CD36-negative platelets exhibit a mild defect in the initial stages of adhesion to fibrillar collagen I (ref. 38). Notably, VLDL increases platelet response to collagen in a CD36-dependent manner; however, the mechanism of this effect remains unclear³⁹. Platelet CD36 is associated with non-receptor tyrosine kinases of the Src family⁴⁰, which have previously been implicated in platelet activation by oxidized LDL⁴¹. The present findings suggest that platelet CD36 might serve as a sensor of specific oxidized phospholipids generated during oxidative stress, providing a mechanism for CD36 involvement in the prothrombotic phenotype associated with dyslipidemia, oxidant stress and atherosclerosis. CD36 engagement may induce an activating signal that is additive (or synergistic) with signals from other receptors and may result in platelet activation by subthreshold concentrations of physiological agonists. Thus, CD36 joins a growing number of platelet receptors and ligands that may potentiate members of the platelet activation cascade, including Gas6 and its receptors (ref. 42), CD40 ligand and $\alpha_{IIb}\beta_3$ (ref. 43) and Eph kinases and ephrins⁴⁴. Unlike other 'co-receptor' ligands, which are primarily localized to the platelet surface during the initial phase of platelet aggregation, CD36 ligands are likely to be presented to the platelet surface before 'classical' platelet agonists. Thus, CD36 may serve to 'prime' or sensitize the platelet for subsequent activation, and this may contribute to platelet hyperreactivity.

METHODS

Sources of materials

Na[¹²⁵I] was from ICN Pharmaceutical, Inc. Native unoxidized phospholipids were from Avanti Polar Lipids. Anti-CD36 monoclonal antibody FA6-152 was from Immunotech. The Fab fragment of FA6 was generated by papain digestion. Conjugated anti-murine P-selectin and anti-murine activated $\alpha_{IIb}\beta_3$ (clone JON/A) monoclonal antibodies were from Emfret Analytics. Specific anti-human P-selectin murine monoclonal antibody was either generated using purified human platelets as antigen and conjugated to FITC or purchased from BD Biosciences/Pharmingen. FITC-conjugated PAC-1 was from Becton Dickinson. All other reagents were obtained from Sigma Aldrich unless otherwise specified.

Experimental animals

We generated *Cd36*^{-/-} *ApoE*^{-/-} mice by crossing *Cd36*^{-/-} and *ApoE*^{-/-} mice (Taconic) as described³² and established the lines from littermates after crossing heterozygotes, so that all *Cd36*^{-/-} lines were back-crossed six or more times to the C57BL/6 genetic background. The resulting genetic background was 99.22% C57BL/6 and 0.78% 129Sv. Mice were fed normal chow for 4 weeks, followed by a Western diet (cholate-free, 21% (wt/wt) adjusted calories from anhydrous milk fat and 0.2% (wt/wt) cholesterol, Harlan Teklad, TD 88137) for 12 weeks. *Ldlr*^{-/-} *Cd36*^{-/-} mice were generated by crossing *Cd36*^{-/-} and *Ldlr*^{-/-} mice (Jackson Laboratory). At the age of 8–10 weeks, mice were fed a high-fat (18% wt/wt), high-cholesterol (1.125% wt/wt) diet (Research Diets D12108). All strains are background matched. All procedures were approved by the Institutional Animal Care and Use Committee of Cleveland Clinic. Total serum cholesterol was determined as described²¹.

Lipoproteins and phospholipid vesicle preparation and modification

LDL was isolated, labeled with Na[¹²⁵I] and additionally modified as described²⁴. Phospholipid vesicle preparation was performed as described¹⁶. Briefly, we prepared stock solutions (2 mg/ml) of small unilamellar vesicles comprising PLPC or PAPC with varying mol % of synthetic oxidized phospholipids in argon-sparged sodium phosphate buffer (67 mM, pH 7.4) by extruding the mixtures through a 0.1- μ m polycarbonate filter using an Avanti Mini-Extruder Set (Avanti Polar Lipids, Inc.) at 37 °C. For direct binding experiments, we added ³H-labeled dipalmitoylphosphatidylcholine (25 μ Ci/mg) to phospholipids. We generated NO₂-PAPC and NO₂-PLPC by oxidation of PAPC and PLPC vesicles by the MPO – H₂O₂ – NO₂⁻ system²⁴.

Synthesis of phospholipids

We performed total syntheses of the oxidized phospholipids and then purified them by flash silica column chromatography or high-performance liquid chromatography (HPLC), as described elsewhere^{16,26}. We confirmed the structures by multinuclear magnetic resonance and high-resolution mass spectrometry^{16,26}. We routinely analyzed synthetic lipids by HPLC with on-line electrospray ionization tandem mass spectrometry (LC/ESI/MS/MS). If lipids were found to be less than 95% pure, they were re-isolated before use.

Mass spectrometric analysis of phospholipids

We used LC/ESI/MS/MS to separate and to quantify plasma oxPC species^{16,18}. Briefly, we added 4 ng of internal standard, ditetradecyl phosphatidylcholine (DTPC) to 200 μ l plasma and extracted phospholipids three times following the method of Bligh and Dyer as described¹⁶. We rapidly dried combined extracts under nitrogen flow, resuspended them in 120 μ l 85% (vol/vol) methanol and stored them under argon at –80 °C until analysis was performed no more than 24 h later. We introduced 40 μ l of the extract onto a 2690 HPLC

system (Waters) and separated phospholipids through a C18 column (2 × 150 mm, 5 μm octadecyl silane, Phenomenex) under gradient conditions at flow rate of 0.2 ml/min as described^{16,18}. We introduced the HPLC column effluent onto a Micromass Quattro Ultima triple quadrupole mass spectrometer (Micromass) and analyzed it by positive electrospray ionization in the multiple reaction monitoring (MRM) mode. Following collision-induced fragmentation with argon gas, phosphatidylcholine molecules produced a diagnostic product ion with mass-to-charge ratio (m/z) 184, corresponding to the protonated phosphocholine headgroup. The ion pairs for the MRM transitions monitored were each molecular ion [MH]⁺ of the phosphatidylcholines and the diagnostic product ion (m/z 184). We constructed calibration curves with a fixed amount of DTPC and varying amounts of each synthetic phosphatidylcholine.

Intravital thrombosis

We isolated platelets from platelet-rich mouse plasma by gel filtration on a Sepharose 2B column (Sigma-Aldrich), then fluorescently labeled platelets with calcein (Molecular Probes) and injected them into syngeneic male mice (4–5 × 10⁶ platelets per g) via the lateral tail vein. We exposed the vessel of choice in mice anesthetized with ketamine and xylazine, visualized mesenteric arterioles (50–80 μm in diameter) or venules (60–80 μm diameter) or the carotid artery on a Leica DM LFS microscope with water immersion objectives and recorded images with a high-speed, color, cooled digital camera (QImaging Retiga EXi Fast 1394) with Streampix high-speed acquisition software. We recorded the resting blood vessel for 3 min, then created a vessel-wall injury by application of a 1.5 × 1.5 mm square of Whatman filter paper soaked in FeCl₃ solution to the surface of the vessel (we used 12.5% FeCl₃ for 3 min on mesenteric vessels and 10% FeCl₃ for 2 min on carotid arteries in hyperlipidemic animals; we increased FeCl₃ exposure times by 1 min in chow diet-fed animals). Then we removed the paper, covered the vessel with saline at 37 °C and recorded platelet vessel wall interactions for 30 min, or until full occlusion occurred and lasted for more than 30 s. Experiments with platelet depleted mice were performed as follows. *Apoe*^{-/-} mice and *Apoe*^{-/-} *Cd36*^{-/-} mice on a Western diet were depleted of platelets by γ-irradiation (11 Gy) and when platelet counts dropped below 5% of normal the mice were injected with 12.5 × 10⁶/g body weight platelets from either *Apoe*^{-/-} mice ($n = 5$) or *Apoe*^{-/-} *Cd36*^{-/-} mice ($n = 5$). Carotid artery occlusion test was performed by application of 15% FeCl₃ for 3 min.

Clinical samples

All human blood products were obtained using protocols approved by the Institutional Review Boards of the Cleveland Clinic and The Blood Center of Wisconsin. Informed consent was obtained from all donors.

Statistical analysis

In most assays, we used the two-sample *t*-test to evaluate statistical significance. In intravital thrombosis experiments, we used the nonparametric log-rank test. Spearman's correlation coefficient was calculated with GraphPad Prism 4.0c.

Supplementary Material

Refer to Web version on PubMed Central for supplementary material.

Acknowledgments

We thank E. Plow for thoughtful comments and criticisms and W. Feng, W. Li and V. Verbovetskaya for technical assistance. This work was supported in part by National Institutes of Health grants HL077213 and HL053315

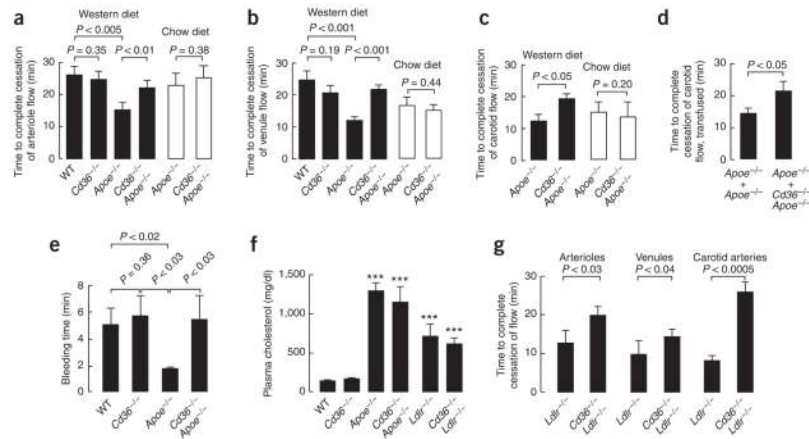
(E.A.P.) and by a Scientist Development Grant from the American Heart Association (E.A.P.), HL70621 and HL076491 (S.L.H.), HL 70083 (M.F.), HL072942 and HL46403 (R.L.S. and M.F.), HL071625, HL073311 and HL077107 (T.V.B.), HL53315 (R.G.S.), Cleveland Clinic Specialized Centers for Clinically Oriented Research (P01 HL077107, S.L.H.; and P50 HL81011, R.L.S. and M.F.) and the Cleveland Clinic Foundation General Clinical Research Center (M01 RR018390).

References

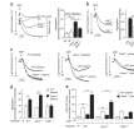
1. Trip MD, Cats VM, van Capelle FJ, Vreken J. Platelet hyperreactivity and prognosis in survivors of myocardial infarction. *N Engl J Med* 1990;322:1549–1554. [PubMed: 2336086]
2. Lacoste L, et al. Hyperlipidemia and coronary disease. Correction of the increased thrombogenic potential with cholesterol reduction. *Circulation* 1995;92:3172–3177. [PubMed: 7586300]
3. Kabbani SS, et al. Platelet reactivity characterized prospectively: a determinant of outcome 90 days after percutaneous coronary intervention. *Circulation* 2001;104:181–186. [PubMed: 11447083]
4. Vanschoonbeek K, et al. Thrombin-induced hyperactivity of platelets of young stroke patients: involvement of thrombin receptors in the subject-dependent variability in Ca²⁺ signal generation. *Thromb Haemost* 2002;88:931–937. [PubMed: 12529741]
5. Kabbani SS, et al. Usefulness of platelet reactivity before percutaneous coronary intervention in determining cardiac risk one year later. *Am J Cardiol* 2003;91:876–878. [PubMed: 12667577]
6. Carvalho AC, Colman RW, Lees RS. Platelet function in hyperlipoproteinemia. *N Engl J Med* 1974;290:434–438. [PubMed: 4359434]
7. Stuart MJ, Gerrard JM, White JG. Effect of cholesterol on production of thromboxane b2 by platelets in vitro. *N Engl J Med* 1980;302:6–10. [PubMed: 7350406]
8. Davi G, et al. Increased thromboxane biosynthesis in type IIa hypercholesterolemia. *Circulation* 1992;85:1792–1798. [PubMed: 1572035]
9. Davi G, et al. Increased levels of soluble P-selectin in hypercholesterolemic patients. *Circulation* 1998;97:953–957. [PubMed: 9529262]
10. Cipollone F, et al. Association between enhanced soluble CD40L and prothrombotic state in hypercholesterolemia: effects of statin therapy. *Circulation* 2002;106:399–402. [PubMed: 12135935]
11. Wang TH, Bhatt DL, Topol EJ. Aspirin and clopidogrel resistance: an emerging clinical entity. *Eur Heart J*. 2005
12. Salonen JT, et al. Effects of antioxidant supplementation on platelet function: a randomized pair-matched, placebo-controlled, double-blind trial in men with low antioxidant status. *Am J Clin Nutr* 1991;53:1222–1229. [PubMed: 1826987]
13. Vericel E, Januel C, Carreras M, Moulin P, Lagarde M. Diabetic patients without vascular complications display enhanced basal platelet activation and decreased antioxidant status. *Diabetes* 2004;53:1046–1051. [PubMed: 15047620]
14. Morita H, Ikeda H, Haramaki N, Eguchi H, Imaizumi T. Only two-week smoking cessation improves platelet aggregability and intraplatelet redox imbalance of long-term smokers. *J Am Coll Cardiol* 2005;45:589–594. [PubMed: 15708708]
15. Berliner JA, Watson AD. A role for oxidized phospholipids in atherosclerosis. *N Engl J Med* 2005;353:9–11. [PubMed: 16000351]
16. Podrez EA, et al. Identification of a novel family of oxidized phospholipids that serve as ligands for the macrophage scavenger receptor CD36. *J Biol Chem* 2002;277:38503–38516. [PubMed: 12105195]
17. Podrez EA, et al. A novel family of atherogenic oxidized phospholipids promotes macrophage foam cell formation via the scavenger receptor CD36 and is enriched in atherosclerotic lesions. *J Biol Chem* 2002;277:38517–38523. [PubMed: 12145296]
18. Sun M, et al. Light-induced oxidation of photoreceptor outer segment phospholipids generates ligands for CD36-mediated phagocytosis by retinal pigment epithelium: a potential mechanism for modulating outer segment phagocytosis under oxidant stress conditions. *J Biol Chem* 2006;281:4222–4230. [PubMed: 16354659]

19. Podrez EA, et al. Macrophage scavenger receptor CD36 is the major receptor for LDL modified by monocyte-generated reactive nitrogen species. *J Clin Invest* 2000;105:1095–1108. [PubMed: 10772654]
20. Febbraio M, Hajjar DP, Silverstein RL. CD36: a class B scavenger receptor involved in angiogenesis, atherosclerosis, inflammation, and lipid metabolism. *J Clin Invest* 2001;108:785–791. [PubMed: 11560944]
21. Febbraio M, et al. Targeted disruption of the class B scavenger receptor CD36 protects against atherosclerotic lesion development in mice. *J Clin Invest* 2000;105:1049–1056. [PubMed: 10772649]
22. Tandon NN, Lipsky RH, Burgess WH, Jamieson GA. Isolation and characterization of platelet glycoprotein IV (CD36). *J Biol Chem* 1989;264:7570–7575. [PubMed: 2468669]
23. Hoebe K, et al. CD36 is a sensor of diacylglycerides. *Nature* 2005;433:523–527. [PubMed: 15690042]
24. Podrez EA, Schmitt D, Hoff HF, Hazen SL. Myeloperoxidase-generated reactive nitrogen species convert LDL into an atherogenic form in vitro. *J Clin Invest* 1999;103:1547–1560. [PubMed: 10359564]
25. Kieffer N, et al. Developmentally-regulated expression of a 78-kDa erythroblast membrane glycoprotein immunologically related to the platelet thrombospondin receptor. *Biochem J* 1989;262:835–842. [PubMed: 2480109]
26. Watson AD, et al. Structural identification by mass spectrometry of oxidized phospholipids in minimally-oxidized low-density lipoproteins that induce monocyte/endothelial interactions and evidence for their presence *in vivo*. *J Biol Chem* 1997;272:13597–13607. [PubMed: 9153208]
27. Boullier A, et al. Phosphocholine as a pattern recognition ligand for CD36. *J Lipid Res* 2005;46:969–976. [PubMed: 15722561]
28. Simon DI, et al. Decreased neointimal formation in *Mac1^{-/-}* mice reveals a role for inflammation in vascular repair after angioplasty. *J Clin Invest* 2000;105:293–300. [PubMed: 10675355]
29. Sarma J, et al. Increased platelet binding to circulating monocytes in acute coronary syndromes. *Circulation* 2002;105:2166–2171. [PubMed: 11994250]
30. Huo Y, et al. Circulating activated platelets exacerbate atherosclerosis in mice deficient in apolipoprotein E. *Nat Med* 2003;9:61–67. [PubMed: 12483207]
31. Pearce SF, et al. Recombinant glutathione *S*-transferase/CD36 fusion proteins define an oxidized low-density lipoprotein-binding domain. *J Biol Chem* 1998;273:34875–34881. [PubMed: 9857015]
32. Febbraio M, Guy E, Silverstein RL. Stem cell transplantation reveals that absence of macrophage CD36 is protective against atherosclerosis. *Arterioscler Thromb Vasc Biol* 2004;24:2333–2338. [PubMed: 15486305]
33. Eitzman DT, Westrick RJ, Xu Z, Tyson J, Ginsburg D. Hyperlipidemia promotes thrombosis after injury to atherosclerotic vessels in apolipoprotein E-deficient mice. *Arterioscler Thromb Vasc Biol* 2000;20:1831–1834. [PubMed: 10894825]
34. Schafer K, et al. Enhanced thrombosis in atherosclerosis-prone mice is associated with increased arterial expression of plasminogen activator inhibitor-1. *Arterioscler Thromb Vasc Biol* 2003;23:2097–2103. [PubMed: 14512369]
35. Barter PJ, et al. Antiinflammatory properties of HDL. *Circ Res* 2004;95:764–772. [PubMed: 15486323]
36. Bodart V, et al. CD36 mediates the cardiovascular action of growth hormone-releasing peptides in the heart. *Circ Res* 2002;90:844–849. [PubMed: 11988484]
37. Philips JA, Rubin EJ, Perrimon N. *Drosophila* RNAi screen reveals CD36 family member required for mycobacterial infection. *Science* 2005;309:1251–1253. [PubMed: 16020694]
38. Tandon NN, Ockenhouse CF, Greco NJ, Jamieson GA. Adhesive functions of platelets lacking glycoprotein IV (CD36). *Blood* 1991;78:2809–2813. [PubMed: 1720035]
39. Englyst NA, Taube JM, Aitman TJ, Baglin TP, Byrne CD. A novel role for CD36 in VLDL-enhanced platelet activation. *Diabetes* 2003;52:1248–1255. [PubMed: 12716760]

40. Huang MM, Bolen JB, Barnwell JW, Shattil SJ, Brugge JS. Membrane glycoprotein IV (CD36) is physically associated with the Fyn, Lyn, and Yes protein-tyrosine kinases in human platelets. *Proc Natl Acad Sci USA* 1991;88:7844–7848. [PubMed: 1715582]
41. Maschberger P, et al. Mildly oxidized low-density lipoprotein rapidly stimulates via activation of the lysophosphatidic acid receptor Src family and Syk tyrosine kinases and Ca²⁺ influx in human platelets. *J Biol Chem* 2000;275:19159–19166. [PubMed: 10764819]
42. Angelillo-Scherrer A, et al. Deficiency or inhibition of Gas6 causes platelet dysfunction and protects mice against thrombosis. *Nat Med* 2001;7:215–221. [PubMed: 11175853]
43. Andre P, et al. CD40L stabilizes arterial thrombi by a β 3 integrin–dependent mechanism. *Nat Med* 2002;8:247–252. [PubMed: 11875495]
44. Prevost N, et al. Eph kinases and ephrins support thrombus growth and stability by regulating integrin outside-in signaling in platelets. *Proc Natl Acad Sci USA* 2005;102:9820–9825. [PubMed: 15994237]
45. Plow EF, et al. Related binding mechanisms for fibrinogen, fibronectin, von Willebrand factor, and thrombospondin on thrombin-stimulated human platelets. *Blood* 1985;66:724–727. [PubMed: 3875376]

**Figure 1.**

CD36 plays a role in thrombosis *in vivo* in the setting of hypercholesterolemia. (a–c) Mice of the indicated genotypes were maintained on Western diet (solid bars) and then used for an intravital thrombosis assay. Mesenteric arterioles (a) or venules (b) or carotid arteries (c) were visualized, and *in vivo* thrombosis times were measured as described in Methods. Mice on chow diet (empty bars) were analyzed in the same way, except that FeCl₃ exposure times were increased by 1 min. Data are presented as mean ± s.e.m. for $n \geq 7$ for chow diet and $n \geq 8$ for Western diet. (d) *ApoE*^{-/-} mice and *ApoE*^{-/-} *Cd36*^{-/-} on a Western diet were depleted of platelets by γ -irradiation, subsequently injected with platelets from either *ApoE*^{-/-} mice ($n = 5$) or *ApoE*^{-/-} *Cd36*^{-/-} mice ($n = 5$) and the carotid artery occlusion test was performed as described in Methods. (e) Tail vein bleeding assay was performed as described in Methods. Data are presented as mean ± s.e.m.; numbers of mice used are: wild-type ($n = 8$), *Cd36*^{-/-} ($n = 5$), *ApoE*^{-/-} ($n = 4$) and *Cd36*^{-/-} *ApoE*^{-/-} ($n = 4$). (f) Total plasma cholesterol concentration is presented as mean ± s.d. mg/dl for at least 6 animals with the indicated genotype on a Western diet. *** $P < 0.001$ by *t*-test as compared to wild-type. (g) Indicated groups of mice were fed a high-cholesterol diet as described in Methods, and *in vivo* thrombosis times were assessed as in a–c. $n \geq 7$ animals in each group. See Supplementary Methods for details.

**Figure 2.**

CD36 deficiency blunts platelet responses to agonists in hypercholesterolemic plasma. **(a,b)** Platelet aggregation in platelet-rich plasma from mice of the indicated genotypes on the indicated diets was induced by ADP and optically monitored. Representative aggregation curves are shown. Bar graph shows aggregation results expressed as maximal amplitude of aggregation (mean \pm s.e.m.; $n = 3$ for WT, $n = 4$ for *Apoe*^{-/-}, $n = 6$ for *Apoe*^{-/-} *Cd36*^{-/-}, $n = 3$ for *Ldlr*^{-/-} and $n = 4$ for *Ldlr*^{-/-} *Cd36*^{-/-}). **(c)** Platelets were isolated by gel filtration of pooled blood from wild-type and *Cd36*^{-/-} mice on a chow diet and *Apoe*^{-/-} mice on a Western diet as described in Methods. Citrated, pooled, platelet-poor plasma from either wild-type or *Apoe*^{-/-} mice on a Western diet was isolated and combined with platelets of the indicated genotype at a 1:1 ratio. Aggregation was induced by ADP and optically monitored. Representative aggregation curves are shown. **(d)** Bar graph shows aggregation results from **c** expressed as maximal amplitude of aggregation (mean \pm s.e.m.; $n = 3$ for WT, $n = 3$ for *Apoe*^{-/-} and $n = 4$ for *Cd36*^{-/-}). **(e)** Flow cytometric analysis of integrin $\alpha_{IIb}\beta_3$ activation on mouse platelets. Platelets and citrated, platelet-poor plasma were isolated and combined at a 1:2 ratio (vol/vol), stimulated with ADP and integrin $\alpha_{IIb}\beta_3$ activation was assessed using JON/A, a monoclonal, phycoerythrin-conjugated antibody for mouse $\alpha_{IIb}\beta_3$ in the activated conformation (mean \pm s.e.m.; $n = 3$ for WT, $n = 3$ for *Apoe*^{-/-}, $n = 4$ for *Cd36*^{-/-}). * $P < 0.05$, ** $P < 0.01$ and *** $P < 0.001$. See Supplementary Methods for details.

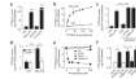


Figure 3.

Platelet CD36 specifically binds oxPC_{CD36} and LDL oxidized by MPO – H₂O₂ – NO₂⁻ system. **(a)** [¹²⁵I]LDL modified by the indicated methods was incubated with platelets isolated from humans in Tyrode's buffer in the presence of 2 mM Ca²⁺ at room temperature. Unbound [¹²⁵I]LDL was separated from platelets and the bound radioactivity was quantified. NO₂-LDL, LDL oxidized by the MPO-H₂O₂-NO₂⁻ system; AcetLDL, acetylated LDL; Cu-oxLDL, Cu²⁺-oxidized LDL. **(b)** Concentration dependence of [¹²⁵I]NO₂-LDL binding by platelets. Binding of [¹²⁵I]LDL was used as a control. **(c)** Human platelets were fixed with paraformaldehyde⁴⁵ and incubated with [¹²⁵I]NO₂-LDL in the presence or absence of the indicated antibodies (20 μg/ml), and the bound radioactivity was assessed. **(d)** Binding of native [¹²⁵I]LDL and [¹²⁵I]NO₂-LDL by isolated platelets from *Cd36*^{-/-} and wild-type mice was assessed as in **a**. **(e)** Binding of [¹²⁵I]NO₂-LDL to human platelets in the presence of various concentrations of the indicated phospholipids was determined as in **a**. **(f)** Direct binding of vesicles containing 40 mol % of PAPC (for KOOA-PC) or 40 mol % of PLPC (for KODA-PC), 40 mol % of the indicated specific native phospholipid or oxPC_{CD36}, 20 mol % of cholesterol, and trace amounts of [3H]DPPC (1,2-dihexadecanoyl-*sn*-glycero-3-phosphocholine) were generated and then incubated with platelets alone or, in the case of KODA-PC-containing vesicles, in the presence of either CD36-specific monoclonal antibody (FA6) or nonimmune, isotype-matched antibody (NI IgG). Unbound vesicles were separated and platelet-bound radioactivity was then quantified. Results represent the mean ± s.d. of three independent experiments. **P* < 0.05, ***P* < 0.01 and ****P* < 0.001. See Supplementary Methods for details.

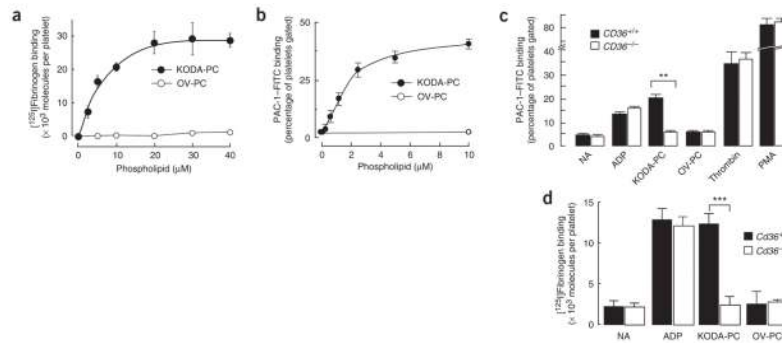


Figure 4. oxPC_{CD36} activates platelet fibrinogen receptor integrin $\alpha_{\text{IIb}}\beta_3$ in a CD36-dependent manner. **(a)** Human platelets isolated by gel filtration were incubated with increasing concentrations of oxPC_{CD36} or OV-PC and $\alpha_{\text{IIb}}\beta_3$ activation was assessed on the basis of the binding of ^{125}I -labeled fibrinogen. **(b)** Human platelets isolated by gel filtration were incubated with increasing concentrations of oxPC_{CD36} or OV-PC. After addition of agonist, FITC-labeled PAC-1 mouse monoclonal antibody (specific for activated integrin $\alpha_{\text{IIb}}\beta_3$) was added at a dilution of 1:100 and $\alpha_{\text{IIb}}\beta_3$ activation was assessed by FACS analysis. **(c)** Human platelets were isolated from CD36^{+/+} or CD36^{-/-} donors and analyzed for $\alpha_{\text{IIb}}\beta_3$ activation as in **b**. The final concentrations of stimuli used were 10 μM ADP, 20 μM lipid oxidized phospholipids, 0.5 U/ml thrombin and 10 nM PMA. NA, no additions. **(d)** Washed platelets from wild-type or *Cd36*^{-/-} mice were incubated with 10 μM ADP or 20 μM synthetic oxidized phospholipids, and platelet activation was assessed by ^{125}I -labeled fibrinogen binding. NA, no additions. Results represent the mean \pm s.d. of three independent experiments. Statistical significance was determined by *t*-test: **P* < 0.05, ***P* < 0.01, ****P* < 0.001. See Supplementary Methods for details.

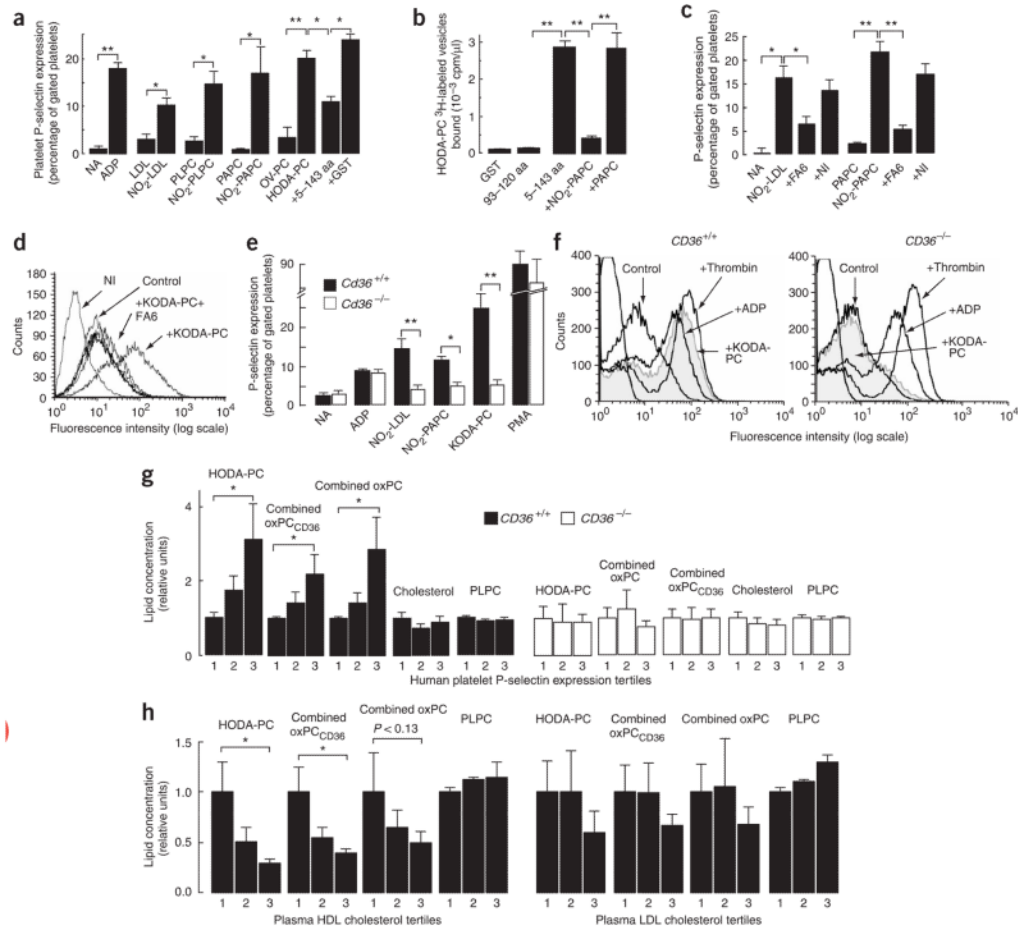
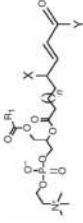


Figure 5. oxPC_{CD36} induce platelet P-selectin expression in a CD36-dependent manner. **(a)** Isolated human platelets were incubated with the indicated stimuli and P-selectin expression was assessed as described in Methods. NA, no additions. Results represent the mean \pm s.d. of three independent experiments. 5–144 aa, CD36-GST fusion peptide with amino acids 5–144 of CD36; GST, glutathione *S*-transferase. **(b)** Binding of ³H-labeled small unilamellar vesicles containing oxPC_{CD36} (HODA-PC) to recombinant CD36-GST fusion peptides immobilized on glutathione-Sepharose was assessed in the presence or absence of the indicated competitors. 93–120 aa, CD36-GST fusion peptide with amino acids 93–120 of CD36. **(c,d)** Effect of the Fab fragment of the CD36-blocking monoclonal antibody on platelet activation induced by **(c)** NO₂-LDL and NO₂-PAPC and **(d)** oxPC_{CD36}. NI, nonimmune isotype-matched antibody. **(e)** Platelet P-selectin expression was determined using FITC-conjugated antibody to mouse P-selectin. **(f)** Human platelets isolated from CD36^{+/+} or CD36^{-/-} donors were treated with agonists and P-selectin expression was assessed. **(b,c,e)** Data are presented as mean \pm s.d. of three independent experiments; **(d,f)** data are presented as a typical result of at least three independent experiments. **(g)** Human platelets from CD36^{+/+} or CD36^{-/-} donors ($n = 3$) were combined with human citrated plasma from various donors, stimulated with ADP, and P-selectin expression was assessed. Samples were divided into tertiles according to P-selectin expression, the mean plasma sample lipid levels were assigned a relative value of 1 for the lowest P-selectin tertile, and the means \pm s.e.m. are shown for all P-selectin tertiles. **(h)** Human plasma samples ($n = 24$) were analyzed for levels of multiple oxidized phospholipids, HDL cholesterol and LDL

cholesterol. Samples were divided into tertiles according to HDL cholesterol or LDL cholesterol concentrations. The mean oxidized phospholipid levels were assigned relative values of 1 for the lowest lipoprotein tertile, and corresponding mean \pm s.e.m. are shown for all lipoprotein tertiles. * $P < 0.05$, ** $P < 0.01$, *** $P < 0.001$. See Supplementary Methods for details.

Table 1

oxPCD₃₆ are markedly increased in the plasma of mice fed a diet enriched in cholesterol

							PL-PC, n = 5					
	HODiA	KODiA	HOOA	KOOA	HDdiA	KDdiA	HODA	KODA	HODiA-PC X-OH, Y=OH	KODiA-PC X-O, Y=OH	HODiA-PC X-OH, Y=OH	KODiA-PC X-O, Y=OH
Chow, WT (n = 5)	0.06 ± 0.02	0.28 ± 0.05	0.36 ± 0.07	0.06 ± 0.01	0.04 ± 0.01	0.04 ± 0.01	0.10 ± 0.02	0.17 ± 0.08				
Chow, <i>Apoe</i> ^{-/-} (n = 5)	0.16 ± 0.14	0.67 ± 0.54	0.44 ± 0.39	0.17 ± 0.19	0.25 ± 0.14	0.30 ± 0.23	0.32 ± 0.22	0.50 ± 0.42				
Western, <i>Apoe</i> ^{-/-} (n = 5)	0.64 ± 0.13	3.00 ± 0.62	0.66 ± 0.10	1.82 ± 0.20	1.15 ± 0.50	1.38 ± 0.68	1.11 ± 0.21	2.26 ± 0.10				
Fold increase over WT	10.7	10.7	1.8	30.3	28.8	34.5	11.1	13.3				
<i>P</i> value of increase	<i>P</i> < 0.0001	<i>P</i> < 0.0001	<i>P</i> < 0.0006	<i>P</i> < 0.0001	<i>P</i> < 0.001	<i>P</i> < 0.002	<i>P</i> < 0.0001	<i>P</i> < 0.0001				
Chow, <i>Ldlr</i> ^{-/-} (n = 8)	0.10 ± 0.08	0.40 ± 0.20	0.39 ± 0.22	0.13 ± 0.08	0.11 ± 0.06	0.16 ± 0.11	0.30 ± 0.16	0.24 ± 0.16				
Western, <i>Ldlr</i> ^{-/-} (n = 5)	0.60 ± 0.24	2.21 ± 0.56	1.70 ± 0.87	0.56 ± 0.17	0.50 ± 0.26	0.79 ± 0.30	1.63 ± 0.35	1.44 ± 0.66				
Fold increase over <i>Ldlr</i> ^{-/-} , chow	6.0	5.5	4.4	4.3	4.5	4.9	5.4	6.0				
<i>P</i> value of increase	<i>P</i> < 0.0002	<i>P</i> < 0.0001	<i>P</i> < 0.001	<i>P</i> < 0.0001	<i>P</i> < 0.001	<i>P</i> < 0.0002	<i>P</i> < 0.0001	<i>P</i> < 0.0004				

The plasma concentrations of the indicated oxidized PC species (in μmol/l) in overnight-fasted, age-matched males fed chow or Western diet for 12 weeks were determined by LC/ESI/MS/MS analysis as described in Methods. Data are expressed as mean ± s.d. for 5–8 animals in each group. Abbreviations: HDdiA-PC and HODiA-PC, the 9-hydroxy-10-dodecenoic acid and 5-hydroxy-8-oxo-6-octenedioic acid esters of 2-lysoPC; HODiA-PC and HOOA-PC, the 9-hydroxy-12-oxo-10-dodecenoic acid and 5-hydroxy-8-oxo-6-octenoic acid esters of 2-lysoPC; KODiA-PC and KOOA-PC, the 9-keto-12-oxo-10-dodecenoic acid and 5-keto-8-oxo-6-octenoic acid esters of 2-lysoPC; KDdiA-PC and KODiA-PC, the 9-keto-10-dodecenoic acid and 5-keto-6-octenedioic acid esters of 2-lysoPC; WT, wild type.